This document is a preprint of: A.B. Martinez, A. Kumar, M. Chafii et al., "A New Approach for Accurate Time Synchronization Using Chirp Signals," in Proceedings of IEEE Vehicular Technology Conference (VTC Spring 2020), Antwerp, Belgium, (pp. 1-5), May 2020. DOI:10.1109/VTC2020-Spring48590.2020.9128652

A New Approach for Accurate Time Synchronization Using Chirp Signals

Ana Belen Martinez*, Atul Kumar*, Marwa Chafii†, Gerhard Fettweis*

*Vodafone Chair Mobile Communications Systems, Technische Universität Dresden, Germany
{ana-belen.martinez,atul.kumar,fettweis}@ifn.et.tu-dresden.de

†ETIS, CY Université, ENSEA, CNRS, F-95000, Cergy, France
marwa.chafii@ensea.fr

***Abstract*—In analog receivers, the use of matched filtering with linear frequency modulated signals constitutes an effective means for detecting the presence of an incoming frame as well as for estimating the symbol timing offset (STO). However, in digital receivers, the discrete nature of the corresponding polyphase codes leads, under certain conditions of carrier frequency offsets, to a significant degradation at the output of the matched filter, which, consequently, can result in erroneous STO estimations. Exploiting the symmetry of a reference sequence consisting of a polyphase code and its complex conjugate, this work proposes a new algorithm based on reversed autocorrelation (RC) to improve the accuracy of the STO estimation obtained by matched filtering. On the one hand, the theoretical analysis demonstrates the superiority of matched filtering over RC in terms of detection performance in the low signal-to-noise ratio regime. On the other hand, it is shown by means of numerical evaluation that the RC can efficiently resolve the STO estimation ambiguity.**

***Index Terms*—symbol timing offset, carrier frequency offset, polyphase code, matched filter, reversed autocorrelation**

I. Introduction

Synchronization is one of the most critical procedures to be performed at the receiver of a communication system. The synchronizer is responsible for the detection of an incoming frame as well as for the estimation and compensation of important synchronization parameters, such as time and frequency offsets.

Under additive white Gaussian noise (AWGN) channel conditions, the optimum detector for a known deterministic signal is the matched filter (MF). It maximizes the signal-to-noise ratio (SNR) and the probability of detection for a given probability of false alarm [1]. However, in the presence of unknown parameters, such as carrier frequency offsets (CFOs), a filter matched to the transmitted signal does not correspond to the optimum detector. As a consequence, the MF metric experiences a performance degradation that depends on the characteristics of the reference signal. It has been shown that linear frequency modulated signals or chirps are CFO tolerant and therefore a suitable option as reference signals for an MF-based detection in environments with potentially high CFOs [2].

Using a reference signal composed of a linear chirp followed by its complex conjugate, the estimation of the symbol timing offset (STO) and the CFO can be accomplished based on the coupling between time and frequency offsets obtained at the outputs of the corresponding MFs [3]. However, due to sampling in a digital receiver, certain CFO values can lead to a significant degradation of the MF metric that may compromise the accuracy of the STO estimation.

Reversed autocorrelation (RC) is an approach that exploits the existence of time reversed complex symmetry in the reference signal for fine STO estimation [4]. In [5], an RC-based approach is applied for accurate time synchronization, making use of the symmetry properties of a reference signal generated by the concatenation of one up-chirp and the corresponding down-chirp. This approach, although robust against CFO, suffers from noise amplification due to the multiplication of received samples, and therefore, it cannot provide a reliable STO estimation in the low SNR regime.

Considering the individual strengths of MF and RC, this work proposes a new approach for time synchronization that improves the STO estimation accuracy obtained by matched filtering, while ensuring a high probability of detection in low SNR operating conditions. The theoretical probabilities of detection achievable with MF and RC under the presence of time and frequency offsets are derived and their validity is discussed. Finally, numerical results are shown to corroborate the efficiency of the proposed algorithm in solving the estimation ambiguity inherent in an MF-based approach.

The rest of the paper is organized as follows: Section II introduces the system model, the reference sequence and the general detection strategy. In Section III and Section IV, the detection and STO estimation approaches corresponding to MF and RC are reviewed and their theoretical detection probabilities are derived. The proposed time synchronization approach is presented in Section V, whilst Section VI evaluates its performance. Finally, Section VII concludes the paper.

II. System Model

The received baseband signal in discrete time domain can be described as

$$\begin{aligned} \mathcal{H}_0 &: r[n] = w[n], \\ \mathcal{H}_1 &: r[n] = hx[n-\theta]e^{j2\pi\epsilon n} + w[n], \end{aligned} \tag{1}$$

where the hypotheses $\mathcal{H}_0$ and $\mathcal{H}_1$ account for the absence or presence of the reference sequence $x[n]$, respectively; $w[n]$ denotes complex AWGN with zero mean and variance σ_n^2; $h = |h|e^{j\phi}$ represents the complex channel gain, unknown but constant over the transmission of the reference sequence;

This document is a preprint of: A.B. Martinez, A. Kumar, M. Chafii et al., "A New Approach for Accurate Time Synchronization Using Chirp Signals," in Proceedings of IEEE Vehicular Technology Conference (VTC Spring 2020), Antwerp, Belgium, (pp. 1-5), May 2020. DOI:10.1109/VTC2020-Spring48590.2020.9128652

the STO θ is normalized by the sampling time and modeled as an integer number, whilst the CFO ϵ is normalized by the sampling frequency.

A. Reference Sequence

The reference sequence considered in this work can be expressed as

$$x[n] = \begin{cases} s_u[n], & n = 0, 1, ..., N-1, \\ s_u^*[n-N], & n = N, N+1, ..., 2N-1, \end{cases} \tag{2}$$

where $s_u[n]$ corresponds to a polyphase code P4 [6] with linearly increasing frequency and it is given by

$$s_u[n] = e^{j\pi\left(\frac{n^2}{N} - n\right)}, \tag{3}$$

where N is the length of the sequence in samples. Hereinafter, $s_u^*[n]$, the complex conjugate of $s_u[n]$, is denoted as $s_d[n]$, and the sequences $s_u[n]$ and $s_d[n]$ are referred to as up- and down-chirps, in view of their similarities with the corresponding continuous time linear up- and down-chirps.

Since the reference sequence has unity power, the SNR at the receiver under hypothesis $\mathcal{H}_1$ can be defined as $\text{SNR} = |h|^2/\sigma_n^2$.

B. Test Statistic

The detection strategy involves comparing the test statistic T, defined as the absolute value of a certain metric at its maximum, to a predefined threshold γ. The correct hypothesis is chosen based on the result of the comparison:

$$\begin{aligned} \mathcal{H}_0: &\quad T < \gamma, \\ \mathcal{H}_1: &\quad T \geqslant \gamma. \end{aligned}$$

The test statistics, the corresponding thresholds and the STO estimation algorithms associated to the MF- and RC-based metrics are described in the following sections.

III. Matched Filtering

In MF-based detection, the received signal is filtered with a filter that is matched to the transmitted signal. Given the structure of the reference sequence defined in (2), two different MFs can be applied. In this section, the matched filtering process associated to each component of the reference sequence is explained. Whilst for the STO estimation, the outputs of both MFs are needed, only one MF is required for frame detection. With focus on the MF matched to the up-chirp $s_u[n]$, its output is analyzed in detailed and used as the basis for the derivation of the theoretical detection probability.

A. Metrics

Under the assumption of causality, the impulse response of the filter matched to the sequence $s_p[n]$ can be formulated as

$$g_p[n] = s_p^*[N-1-n], \tag{4}$$

where $p \in \{u, d\}$. In the presence of $x[n]$, filtering the received sequence $r[n]$ with $g_u[n]$ and $g_d[n]$ provides the outputs

$$M_{MF,u}[n] = M_{MF,u,u}[n] + M_{MF,u,d}[n] + w_u[n], \tag{5}$$

$$M_{MF,d}[n] = M_{MF,d,u}[n] + M_{MF,d,d}[n] + w_d[n], \tag{6}$$

where

$$M_{MF,p,u}[n] = \sum_{k=-\infty}^{\infty} h s_u[k-\theta] e^{j2\pi\epsilon k} g_p[n-k], \tag{7}$$

$$M_{MF,p,d}[n] = \sum_{k=-\infty}^{\infty} h s_d[k-N-\theta] e^{j2\pi\epsilon k} g_p[n-k], \tag{8}$$

$$w_p[n] = \sum_{k=-\infty}^{\infty} w[k] g_p[n-k]. \tag{9}$$

$M_{MF,u,u}[n]$ and $M_{MF,d,d}[n]$ are the terms of interest, which are evaluated below. The cross-terms, $M_{MF,u,d}[n]$ and $M_{MF,d,u}[n]$, represent the interference, which can be considered negligible for large values of N. Finally, $w_u[n]$ and $w_d[n]$ refer to the noise components.

The magnitudes of $M_{MF,u,u}[n]$ and $M_{MF,d,d}[n]$ can be written as

$$|M_{MF,u,u}[n']| = |h|(1-|n'|)N \left| \frac{\text{sinc}\left(N(n'+\epsilon)(1-|n'|)\right)}{\text{sinc}(n'+\epsilon)} \right|, \tag{10}$$

$$|M_{MF,d,d}[n'']| = |h|(1-|n''|)N \left| \frac{\text{sinc}\left(N(n''-\epsilon)(1-|n''|)\right)}{\text{sinc}(n''-\epsilon)} \right|, \tag{11}$$

where

$$n' = \frac{n-(\theta+N-1)}{N} \quad \text{and} \quad n'' = \frac{n-(\theta+2N-1)}{N}. \tag{12}$$

The global maximum of $|M_{MF,u,u}[n']|$ and $|M_{MF,d,d}[n'']|$ can be found at

$$n'_u = \arg\max_{n'} |M_{MF,u,u}[n']|, \tag{13}$$

$$n''_d = \arg\max_{n''} |M_{MF,d,d}[n'']|, \tag{14}$$

respectively. The corresponding indexes n_u and n_d are given by

$$n_u = \theta + N - 1 - [\epsilon N], \tag{15}$$

$$n_d = \theta + 2N - 1 + [\epsilon N], \tag{16}$$

where $[.]$ represents rounding to the nearest integer value, and $[\epsilon N]$ corresponds to the integer part of the CFO, normalized by f_s/N, with sampling frequency f_s.

Considering the effects of rounding, the maximum of the magnitude of $|M_{MF,u,u}[n'_u]|$ can now be expressed as

$$|m(\epsilon)| = |h|\left(1-|\epsilon_r|\right) N \left| \frac{\text{sinc}\left(N(\epsilon-\epsilon_r)\left(1-|\epsilon_r|\right)\right)}{\text{sinc}\left(\epsilon-\epsilon_r\right)} \right|, \tag{17}$$

where $\epsilon_r = [\epsilon\, N]/N$.

Fig. 1 shows the value $|m(\epsilon)|$ (blue) as well as the magnitude of the global maximum obtained at the output of the MF after filtering $s_u[n]$ with the corresponding MF $g_u[n]$ (red), for different values of CFO and in the absence of noise. The length N of the sequence $s_u[n]$ is set to 64 samples.

This document is a preprint of: A.B. Martinez, A. Kumar, M. Chafii et al., "A New Approach for Accurate Time Synchronization Using Chirp Signals," in Proceedings of IEEE Vehicular Technology Conference (VTC Spring 2020), Antwerp, Belgium, (pp. 1-5), May 2020. DOI:10.1109/VTC2020-Spring48590.2020.9128652

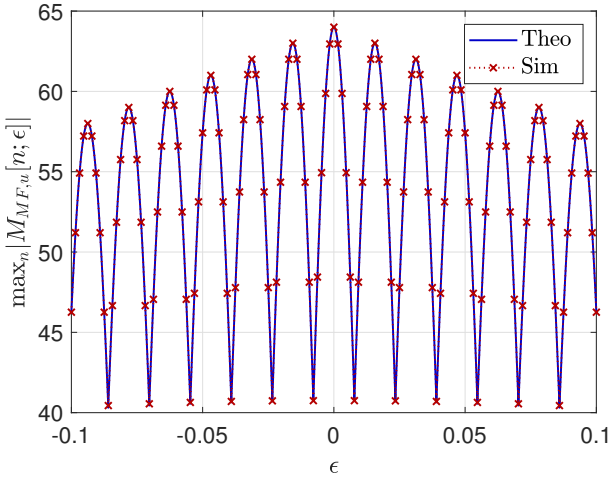

Fig. 1: Theoretical value $|m(\epsilon)|$ and $\max_n |M_{MF,u}[n]|$ obtained through simulations for a sequence $s_u[n]$ of length $N = 64$ samples and in the absence of noise.

B. Test statistic

Considering the output of the MF matched to $s_u[n]$, the test statistic is given by

$$T_{MF} = \max_n |M_{MF,u}[n]|. \tag{18}$$

It can be shown that, under $\mathcal{H}_0$ and $\mathcal{H}_1$, T_{MF} is distributed according to a Rayleigh and a Rician distribution, respectively. Hence,

$$T_{MF} \sim \begin{cases} \text{Rayleigh}\left(\sigma_{_{MF}}\right), & \text{under } \mathcal{H}_0, \\ \text{Rician}\left(|m(\epsilon)|, \sigma_{_{MF}}\right), & \text{under } \mathcal{H}_1, \end{cases} \tag{19}$$

where

$$\sigma_{_{MF}} = \sqrt{N/2}\,\sigma_{_n}. \tag{20}$$

The probabilities of false alarm and detection can be expressed as

$$P_{FA,_{MF}} = Q_{\chi_2^2}\left(\frac{\gamma_{_{MF}}^2}{\sigma_{_{MF}}^2}\right), \quad P_{D,_{MF}}(\epsilon) = Q_{\chi_2'^2(\lambda)}\left(\frac{\gamma_{_{MF}}^2}{\sigma_{_{MF}}^2}\right), \tag{21}$$

where $\lambda = |m(\epsilon)|^2/\sigma_{_{MF}}^2$. The functions $Q_{\chi_2^2}(.)$ and $Q_{\chi_2'^2(\lambda)}(.)$ denote the right-tail probabilities of central and non-central chi-squared random variables with 2 degrees of freedom, respectively. The decision threshold $\gamma_{_{MF}}$ used to select among the hypotheses can be described in terms of the $P_{FA,_{MF}}$ as

$$\gamma_{_{MF}} = \sqrt{-N\sigma_{_n}^2 \ln(P_{FA,_{MF}})}. \tag{22}$$

The probability of detection derived above depends on a deterministic CFO value ϵ. For randomly distributed ϵ, with probability density function $p(\epsilon)$, a new probability of detection can be derived as

$$P_{D,_{MF}} = \int_{\epsilon_{min}}^{\epsilon_{max}} P_{D,_{MF}}(\epsilon)\, p_\epsilon(\epsilon)\, d\epsilon. \tag{23}$$

C. Symbol Timing Offset Estimation

The STO can be estimated using the indexes n_u and n_d, defined in (15) and (16), respectively, as

$$\hat{\theta}_{MF} = \frac{n_u + n_d - 3N + 2}{2}. \tag{24}$$

IV. Reversed Autocorrelation

Exploiting the central symmetry generated by the concatenation of an up- and a down-chirp in the reference sequence, a metric can be defined for the purposes of frame detection and STO estimation. This section reviews the RC metric, derives the associated theoretical detection probability and presents the STO estimation approach.

A. Metric

The RC metric is defined as

$$M_{RC}[n] = \sum_{k=1}^{N-1} r[n+k]\, r[2N+n-k], \tag{25}$$

where the lower limit of the sum, $k = 1$, has been appropriately selected to only take into account the product terms with the aforementioned symmetry.

B. Test Statistic

The test statistic can be written as

$$T_{RC} = \max_n |M_{RC}[n]|. \tag{26}$$

Based on the central limit theorem, the output of the RC can be approximated by a Gaussian distribution for sufficiently large values of N. Thus, the expected value and variance [7] of the product of independent and identically distributed random variables applies. Based on this assumption, the T_{RC} is distributed according to

$$T_{RC} \sim \begin{cases} \text{Rayleigh}\left(\sigma_{_{RC,0}}\right), & \text{under } \mathcal{H}_0, \\ \text{Rician}\left(|h|^2(N-1), \sigma_{_{RC,1}}\right), & \text{under } \mathcal{H}_1. \end{cases} \tag{27}$$

where

$$\sigma_{_{RC,0}} = \sqrt{\frac{N-1}{2}}\sigma_{_n}^2, \tag{28}$$

$$\sigma_{_{RC,1}} = \sqrt{\frac{N-1}{2}(2|h|^2 + \sigma_{_n}^2)}\sigma_{_n}. \tag{29}$$

False alarm and detection probabilities are given by

$$P_{FA,_{RC}} = Q_{\chi_2^2}\left(\frac{\gamma_{_{RC}}^2}{\sigma_{_{RC,0}}^2}\right), \quad P_{D,_{RC}} = Q_{\chi_2'^2(\lambda)}\left(\frac{\gamma_{_{RC}}^2}{\sigma_{_{RC,1}}^2}\right), \tag{30}$$

where $\lambda = (2(N-1)|h|^4)/(\sigma_{_n}^2(2|h|^2 + \sigma_{_n}^2))$. Hence, the detection probability is independent of the CFO. For a given $P_{FA,_{RC}}$, the decision threshold $\gamma_{_{RC}}$ can be written as

$$\gamma_{_{RC}} = \sqrt{-(N-1)\sigma_{_n}^4 \ln(P_{FA,_{RC}})}. \tag{31}$$

This document is a preprint of: A.B. Martinez, A. Kumar, M. Chafii et al., "A New Approach for Accurate Time Synchronization Using Chirp Signals," in Proceedings of IEEE Vehicular Technology Conference (VTC Spring 2020), Antwerp, Belgium, (pp. 1-5), May 2020. DOI:10.1109/VTC2020-Spring48590.2020.9128652

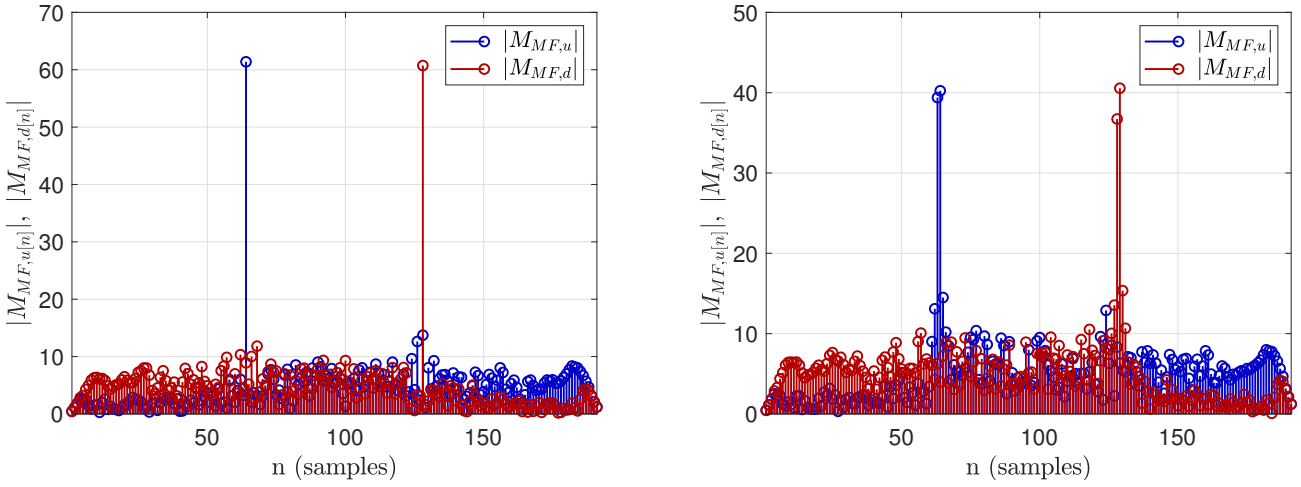

(a) $N\epsilon = 0$ **(b)** $N\epsilon \approx 0.5$

Fig. 2: Magnitude of the outputs of the up- and down-MFs for different values of CFO, normalized by f_s/N. The reference sequence consists of one up-chirp followed by its complex conjugate, each of length $N = 64$ samples. The results are obtained under AWGN channel conditions with SNR $= 10$ dB.

C. Symbol Timing Offset Estimation

The argument of the maximum value at the output of the RC provides an estimate of the STO:

$$\hat{\theta}_{RC} = \arg\max_n |M_{RC}[n]|\,. \tag{32}$$

V. Proposed Approach

The STO estimated by the outputs of the MFs, as described in (24), is subject to inaccuracies due to the presence of noise and fractional frequency offsets (FFOs). The FFO, defined as the fractional part of the CFO normalized by f_s/N, is a major source of degradation of the output of the MFs. This behavior, described by (10) and (11), is exemplified in Fig. 2 for a reference sequence according to (2) with $N = 64$. The global maximum can be clearly identified at the output of each MF when no FFO is present (see Fig. 2 (a)). However, for |FFO| values close to 0.5 two maxima of similar amplitude can be found. Fig. 2 (b) shows that these maxima, contaminated by noise, exhibit fluctuations in their magnitude and cannot be uniquely distinguished. As a consequence, the use of their positions for the STO estimation may lead to wrong values.

The above described situation highlights the potential STO estimation ambiguity. This ambiguity can be detected by examining the estimated value $\hat{\theta}_{MF}$. In fact, the presence of a fractional STO can be considered an indicator of ambiguity and should be the condition that triggers the use of the proposed algorithm. In this case, a sliding window RC with starting indexes given by $\lfloor\hat{\theta}_{MF}\rfloor$, $\lfloor\hat{\theta}_{MF}\rfloor + 1$ and $\lfloor\hat{\theta}_{MF}\rfloor + 2$, are performed. Each individual output is associated to a different correcting offset factor that can be used to refine the initial STO estimate. Requiring the calculation of three RCs, this approach has a computational complexity of $3N - 3$ complex multiplications.

Algorithm 1 lists the key steps of the above-described approach.

Algorithm 1 STO ambiguity resolution

if $\mod(\hat{\theta}_{MF}, 1) \neq 0$ **then**
  sto_code $= [-1\ 0\ 1]$;
  $\theta_{\text{ini}} = \lfloor\hat{\theta}_{MF}\rfloor$;
  rc_vec $= []$;
  for $n = 0$ to 2 **do**
    rc_vec$[n]$ = calculate_rc$(r, \theta_{\text{ini}}, N)$;
    $\theta_{\text{ini}} = \theta_{\text{ini}} + 1$;
  end for
  code_idx $= \arg\max_n |\text{rc\_vec}[n]|$;
  $\lambda =$ sto_code(code_idx);
  $\hat{\theta}_{\text{fine}} = \lfloor\hat{\theta}_{MF}\rfloor + \lambda$;
else
  $\hat{\theta}_{\text{fine}} = \lfloor\hat{\theta}_{MF}\rfloor$;
end if

VI. Simulation Results

In this section, the validity of the derived theoretical detection probabilities and the performance of the proposed algorithm are evaluated. An up-chirp, of length $N = 64$ samples and a bandwidth of 180 kHz, followed by its associated down-chirp, has been used as reference sequence for detection and time synchronization under flat fading channel conditions. For the simulations, a uniformly distributed CFO in the range $[-18, 18]$ kHz has been generated, which, e.g., could represent a transmission at 900 MHz with an accuracy of 20 ppm for the local oscillators. Likewise, the arrival time is considered uniformly distributed, taking integer values from the interval $[0, 10]$ samples. The signal processing is performed at Nyquist

This document is a preprint of: A.B. Martinez, A. Kumar, M. Chafii et al., "A New Approach for Accurate Time Synchronization Using Chirp Signals," in Proceedings of IEEE Vehicular Technology Conference (VTC Spring 2020), Antwerp, Belgium, (pp. 1-5), May 2020. DOI:10.1109/VTC2020-Spring48590.2020.9128652

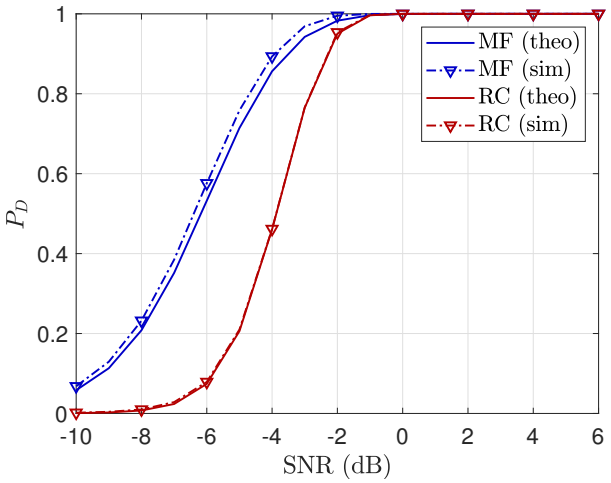

Fig. 3: Probability of detection obtained with MF and RC.

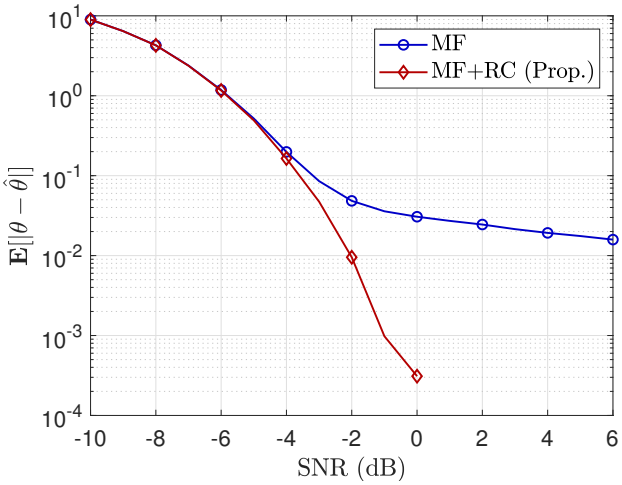

Fig. 4: Mean of the absolute STO estimation error obtained with MFs (blue) and the proposed approach (red).

rate, assuming previous down conversion and subsequent low pass filtering of the received signal.

A constant false alarm rate of 10^{-5} with adaptive decision threshold according to (22) and (31) is considered for every detection approach. Fig. 3 illustrates the theoretical and experimental probabilities of detection associated to MF- and RC-based detection. The simulation results obtained with the RC metric, in red, are in good agreement with the theory, especially in the moderate to high SNR regime, verifying the validity of the theoretical model. For MF-based detection, in blue, a small difference between theory and simulation can be observed. Here, the theoretical results can be considered a lower bound for performance evaluation. The reason for the discrepancy is the correlation introduced in the MF metric by FFO values close to $\pm 0.5 f_s/N$ in the received signal. In accordance with (20) and (29), the effect of noise amplification experienced by the RC yields lower detection performance for small SNR values.

Fig. 4 depicts the STO estimation performance by showing the mean of the absolute STO estimation error for various SNR values. Since the time offset is assumed to be an integer number, the estimation obtained with the MFs according to (24) is truncated to its integer part. Due to the FFO, the MF-based approach cannot provide an error free STO estimation, even at high SNR conditions. The proposed approach is implemented using the estimated $\lfloor \hat{\theta}_{MF} \rfloor$ as a reference. As evident from Fig. 4, it reduces the estimation error in the moderate SNR region and successfully eliminates the STO estimation ambiguity for SNR values above 0 dB.

VII. Conclusions

In this paper, the detection and timing synchronization performance achievable by matched filtering and RC has been analyzed, utilizing the properties of reference sequences that consist of a linear up-chirp followed by its complex conjugate.

The theoretical probability of detection associated to each metric has been derived and their validity has been demonstrated by means of simulations. Whilst theoretical and simulation results exhibit almost perfect coincidence for RC-based detection, they slightly differ for MF-based detection due to the correlation introduced by the FFO. In this case, the analytical expression can be considered a lower bound of detection performance.

The performance evaluation of the proposed approach has shown that the implementation of a sliding window RC with restricted maximum search can successfully eliminate estimation ambiguities inherent in MF-based STO estimation.

Based on the presented evaluation, matched filtering can be recommended for frame detection and STO estimation in the low SNR regime and the alternative RC-based algorithm for high SNR values, where it has proven to be more effective in exploiting the symmetry of the reference sequence.

VIII. Acknowledgment

Authors acknowledge the European Research Council under the European Union's Horizon 2020 Research and Innovation Programme (No. 732174) and the Paris Seine Initiative (ASIA Chair of Excellence Grant).

References

[1] S. M. Kay, *Fundamentals of Statistical Signal Processing. Volume II. Detection Theory*. Upper Saddle River (N.J.): Prentice-Hall, 1998.

[2] J. Zou and C. Xu, "Frequency Offset Tolerant Synchronization Signal Design in NB-IoT," *Sensors*, vol. 18, no. 11, p. 4077, 2018.

[3] S. Boumard and A. Mammela, "Time domain synchronization using Newman chirp training sequences in AWGN channels," in *Proc. IEEE Intern. Conf. Commun. (ICC 2005)*, vol. 2, May 2005, pp. 1147–1151.

[4] T. Bhatt, V. Sundaramurthy, J. Zhang, and D. McCain, "Initial Synchronization for 802.16e Downlink," in *2006 Fortieth Asilomar Conference on Signals, Systems and Computers*, Oct. 2006, pp. 701–706.

[5] S. Boumard and A. Mammela, "Robust and Accurate Frequency and Timing Synchronization Using Chirp Signals," *IEEE Trans. Broadcast.*, vol. 55, no. 1, pp. 115–123, March 2009.

[6] B. L. Lewis and F. F. Kretschmer, "Linear Frequency Modulation Derived Polyphase Pulse Compression Codes," *IEEE Trans. Aerosp. Electron. Syst.*, vol. AES-18, no. 5, pp. 637–641, Sep. 1982.

[7] L. A. Goodman, "On the Exact Variance of Products," *Journal of the American Statistical Association*, vol. 55, no. 292, pp. 708–713, 1960. [Online]. Available: https://www.tandfonline.com/doi/abs/10.1080/01621459.1960.10483369